Investigating the Impact of Construction in Urban Areas on Air Pollution in the Troposphere Using Sentinel Satellite Images: A Case Study in District 22 West of Tehran, Iran

Paniz Nouri [a*], Sara Vahidi [a], Vahid Hatamzadeh [a], Afshin Afshinfar [a] and Shokofeh Karimi [a]

[a] *Iasalmic Azad University, Iran.*

Authors' contributions

This work was carried out in collaboration among all authors. All authors read and approved the final manuscript.

Original Research Article

ABSTRACT

In recent years removing environmental pollution has become one of the main concerns of human life. Air quality in cities depends on weather conditions and the amount of pollutants produced. Today, air pollution is one of the most complex problems of human societies, which has left many negative effects on the health of living beings, especially humans. In this research, the average monthly and annual concentrations of air contaminators in the air pollution measurement stations of the General Directorate of Environmental Protection of Tehran province in the years 2013 to 2019

_____

*Corresponding author: E-mail: paniznouri97@yahoo.com;*

were examined. By using google earth engine site [1]. Processes that GEE (Google Earth Engine) contains a consolidated resource of open-access RS (Remote Sensing) datasets, along with a variety of algorithms to extract information for Earth's surface monitoring [2], and using maximum likelihood classification method it recognized that examining the spatial changes of pollutants in the areas where there was more construction, the amount of contaminators was also higher. In terms of time, however, no special changes have been observed for all gases. For AI (Aerosol Index) pollutant, no very specific changes were observed within the region. We have seen a growing trend for carbon monoxide pollutant. For the nitrogen oxide pollutant, we have not seen any growth during this period of time. For sulfur dioxide, we have seen a growing trend. Also, in terms of seasonal changes, air pollutants are more concentrated in winter.

Keywords: Remote sensing; air pollution; aerosol; sentinel satellite imagery; GEE; maximum likelihood.

1. INTRODUCTION

According to the reports of the World Health Organization, about 7 million people suffer from respiratory diseases every year, which will cause their death .Due to the unique features of remote sensing, i.e. repeatability, comprehensiveness, access to past data, not depending on geographical boundaries, it can be very helpful in discussing air pollution. Atmospheric aerosol exert a profound impact on the climate system [3]. Massive studies have concerned and analyzed driving factors for air contaminators like AI with facilitation of Remote sensing technique, which has become a new means of monitoring global air pollution [4]. Nitrogen dioxide pollution in Khuzestan province was investigated using the TROPOMI sensor in a temporal-spatial way. The concentration of tropospheric NO2 pollution was estimated in each month and the monthly average of the concentration of this pollutant was obtained for Khuzestan province. Finally, the cities and industries of Khuzestan province were prioritized according to the concentration of tropospheric NO2 pollution [5]. The spread of the Covid-19 virus in this period had various consequences that led to a decrease in the activity of factories as well as a decrease in vehicle traffic [6]. In 2020, a spatial-temporal set was presented to measure nitrogen dioxide (NO2). Workflow was reviewed from May 2018 to June 2019. They used Python programming to collect and process data [7]. Nitrogen dioxide pollution was monitored with Sentinel-5 satellite images over Europe. Nitrogen dioxide (NO2) is one of the main air quality pollutants in many cities. In this research, the health status of the society was investigated with tropospheric nitrogen dioxide (NO2) [8]. Urban areas of France were monitored with Sentinel-2 data. Supervised classification and integration were done using Sentinel-2 images to produce more reliable and accurate maps [9]. Sentinel-2

images were used to infiltrate and monitor urban areas. Their main goal has been the integration of multi-temporal and multi-resolution data of Sentinel-2 images [10]. Sentinel-2 images and SVM(Super Vector Machine) algorithm were used to detect buildings. Mapping of urban areas is one of the areas that is investigated with Sentinel-2 data. The ability to use Sentinel-2 data for building recognition is analyzed using SVM algorithm. For their study area, a number of issues including automatic preparation of training data, optimal classifier parameters, and image selection history are analyzed [11]. In 2020, Behrouz Sobhani et al., using Sentinel-5 satellite data, monitored carbon monoxide gas with a spatial-temporal series for health management. They stated that various natural and human factors cause air pollution to affect the health of living beings, especially mental and physical health. To conduct the research, the data of the Sentinel-5 satellite were analyzed in a period of 14 months, with the LST index to monitor daily and nightly temperature changes [12]. In 2019, Siavash et al. investigated the amount of changes in air pollutants during the spread of the Covid-19 virus in Iran using data from the Sentinel-5 satellite. In this research, the temporal and spatial changes of atmospheric pollutants have been determined using Sentinel-5 satellite data in April 2019 at the same time as the spread of the Covid-19 virus in Iran and compared with the values of the same period in 2019. The spread of the Covid-19 virus in this period had various consequences that led to a decrease in the activity of factories as well as a decrease in vehicle traffic. In this research, in order to investigate the effect of the mentioned factors, temporal changes and spatial distribution of pollutants such as air pollution, nitrogen dioxide, carbon monoxide and ozone were analyzed in the interval between these two times. Quantitative and qualitative results show the improvement of air quality in April 2019
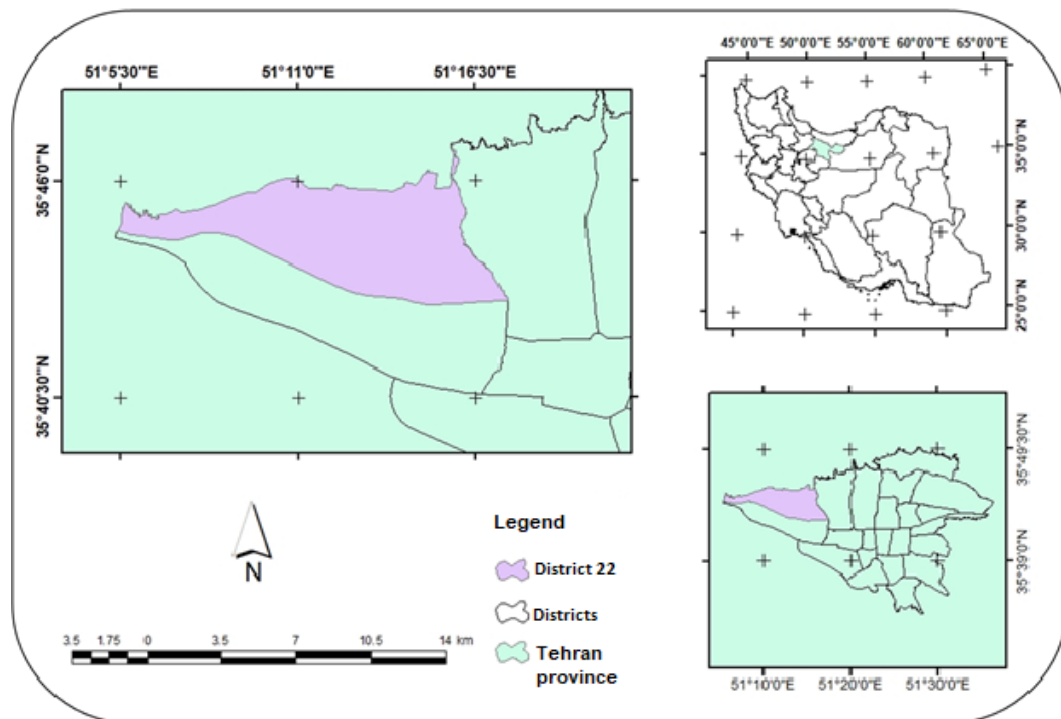
Fig. 1. Study area [14]

compared to the same month last year. Based on the obtained results, the total concentration of nitrogen dioxide in the atmospheric column and nitrogen dioxide in the atmosphere has decreased, which is directly related to transportation and human activities [13]. According to conclusion of recent researches the maximum likelihood method in supervised classification methods has the acceptable capabilities for depict different classes, and there isn't any updated research for important part of metropolis city in Iran District 22 west of Tehran to exhibit influences of recent fast constructions of air pollution, therefore in this study by capabilities of GEE ,ENVI 5.6 software and relying on remote sensing abilities Investigating the relationship between construction in the 22nd district of Tehran on carbon monoxide (CO), sulfur dioxide (SO2), nitrogen dioxide (NO2), tropospheric ozone (O3) and aerosol (AI) pollutants is done by using sentinel-5 satellite images.

1.1 Study Area

The area under study in this research is District 22 of Tehran Municipality. This area, which is located in the northwest of Tehran, can be transformed into an area in accordance with modern urban patterns. The study area is exhibited in Fig. 1.

District 22 of Tehran, today has an area of 5881 hectares are surrounded by towers and arbitrary structures, it could be the last hope of Tehran Municipality to create optimal models of urban planning and urbanization. This area is limited to the Alborz Mountains from the north, the Ken River from the east, the Tehran Karaj Freeway from the south, and the hand-planted forests of Wardvard from the west. This region has an area of 6,200 hectares, of which 1,300 hectares are green spaces. Ali Nuzarpour has been the mayor of this region since 2016. And Chitgar Forest Park covers an area of about 65 hectares of this expanded area. According to the last census conducted in 2010, this area has about 128,958 people, which includes 38,106 households.

2. METHODOLOGY

In this study investigating the impact of construction on air pollution in the troposphere layer using TROPOMI sensor of Sentinel-5 and Sentinel-2 satellites during 2018 to 2022 is done. After downloading cloudless and appropriate sentinel images from GEE(google earth engine), sentinel 2 for land changes and sentinel 5 for estimating of pollution, radiometric atmospherics and geometrics correction had been done in ENVI5.6 image processing software then classification with maximum likelihood method

classification for constructed area have been done. To achieve outperformance after assessing of land changes spatiotemporal parameters had been assessed. Change process of (CO), (NO2), (SO2), (O3), AI (atmospheric aerosol) and seasonal changes contaminators depicts in distinctive maps. For Validity check overall accuracy and kappa coefficient have measured. According to standard definition of these parameters the obtained results are acceptable.

2.1 Accuracy Analysis

After classifying the images, using educational samples that are not involved in the classification process, the validation of the unclassified image is evaluated. ArcGIS methods for spatial information are new technique with high resolution and High reliability.

2.1.1 Overall accuracy

The overall accuracy is obtained from the sum of the main diameter's elements of the error matrix divided by the total number of pixels according to the following equation:

$$\text{Overall Accuracy} = \frac{\sum_{a=1}^{u} c_{aa}}{Q} \times 100 \qquad (1)$$

Where Q and U is the total number of pixels and classes respectively. The minimum acceptable overall accuracy is 85% [15].

2.1.2 Kappa coefficient

The kappa coefficient K is a second measure of classification accuracy which incorporates the off-diagonal element as well as diagonal term to give a more robust assessment of accuracy than overall accuracy it is computed as: [16]

$$k = \frac{\sum_{a=1}^{u} \frac{c_{aa}}{Q} - \sum_{a=1}^{U} \frac{c_a c_a}{Q^2}}{1 - \sum_{a=1}^{U} \frac{c_a c_a}{Q^2}} \qquad (2)$$

Where c_a =row sums

2.2 Implementation of Classification Methods

Image classification methods are divided into 3 groups:

Supervised classification methods, unsupervised classification methods, and object-oriented classification methods [17].

2.2.1 Maximum likelihood classification

One of the most accurate and widely used methods among the various supervised classification methods is the maximum likelihood method. This method evaluates the variance and covariance of different classes. In the maximum likelihood method, it is assumed that all educational regions have a normal distribution function. After evaluating the probabilities in each class, the pixels are assigned to the classes that have the most similarity, and if the probability values are lower than the threshold, they introduce as unclassified pixels [17].

2.3 TROPOMI

The most famous meter in the field of measuring air pollution is the TROPOMI meter. This sensor is also known as Sentinel 5. This satellite captures images in the ultraviolet and infrared ranges. For wavelengths above 300 nm, the harvesting width is 50 km, and for wavelengths below 300 nm, the harvesting width is 8 km. In general, the purpose of this satellite is to measure air quality, monitor stratospheric ozone, measure solar radiation and monitor weather conditions. The first mission of the Copernicus air pollution control program is the construction of Sentinel 5. It is measured to support UV, visible, short-infrared and short-wavelength infrared bands. This satellite is located at an altitude of 824 km and can be useful in detecting ozone, methane, formaldehyde, aerosol, carbon monoxide, NO2, SO2 gases. We can see the specifications of Sentinel-5 bands in Table 1[18].

Table 1. Sentinel5 bands [15]

Band name	Spectral range (nanometer)
UV	270-320
Visible range	310-500
Near infrared	675-775
Short wavelength infrared	2305-2385

Various pollutants can be measured using Sentinel 5 satellite images, including ozone, methane, formaldehyde, aerosol, carbon monoxide, NO2, SO2 [19,20].

2.4 GEE (Google Earth Engine)

GEE contains a consolidated resource of open-access RS datasets, along with a variety of algorithms to extract information for Earth's surface monitoring. This system has a large database of information and images from around

the world that can be easily called up. In this system, you can easily do the necessary processing for different parts of the world and there is no limit. The Google Earth Engine system is a system that users can use on a local to global scale [1].

2.5 Sentinel 2

Sentinel-2 carries the Multispectral Imager (MSI) (Sentinel-2_User_Handbook.pdf). This sensor delivers 13 spectral bands ranging from 10 to 60-meter pixel size, blue (B2), green (B3), red (B4), and near-infrared (B8) channels have a 10-meter resolution.

Next, its red edge (B5), near-infrared NIR (B6, B7, and B8A), and short-wave infrared SWIR (B11 and B12) have a ground sampling distance of 20 meters.

Finally, its coastal aerosol (B1) and cirrus band (B10) have a 60-meter pixel size [16].

3. RESULTS AND DISCUSSION

Based on the method of classification, the construction areas have been identified in this time period and displayed on the map of Fig. 3 and 4. Based on the obtained results, there have been changes in the construction of the region between these 4 years. In Tables 1-4, the results of the overall accuracy and kappa's coefficient

are obtained based on Google Earth images and the results are displayed. Based on the obtained results, the maximum likelihood classification has an average Kappa coefficient of 0.85 and the value is the same.

According to classification by acceptable accuracy which is exhibited in Table 2 About 33 hectares have been added to the construction area. In Tables number 2-4, the construction area and their differences are presented separately. According to the results, the area of construction areas in 2018 is equivalent to 348 hectares and for 2022 it is equivalent to 382 hectares.

According to the standard amount of overall accuracy and kappa coefficient which gives in USGS these numbers are acceptable.

After examining the construction changes, examine the changes of different parameters in the unit of time and space is done. The results of each parameter are shown below. Aerosols are substances suspended in the air caused by human activities or fine dust. These things will land on the ground (of course, if the diameter is more than 100 microns). Monitoring this pollutant is valuable in many studies. Fig. 5 demonstrates the average value of AI. According to this map, the concentration of this gas is higher in the northern, western and southern parts.
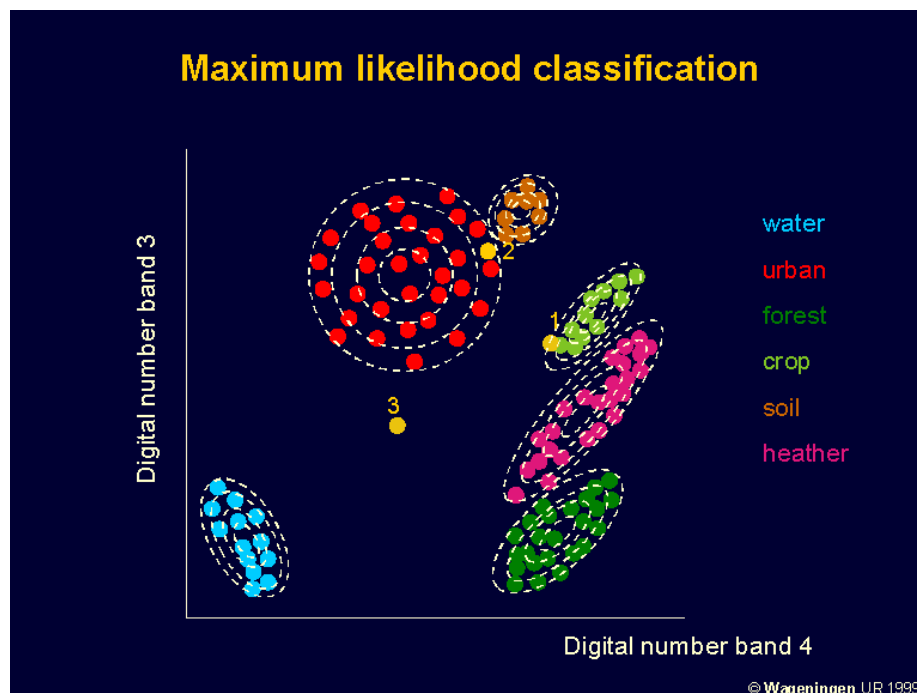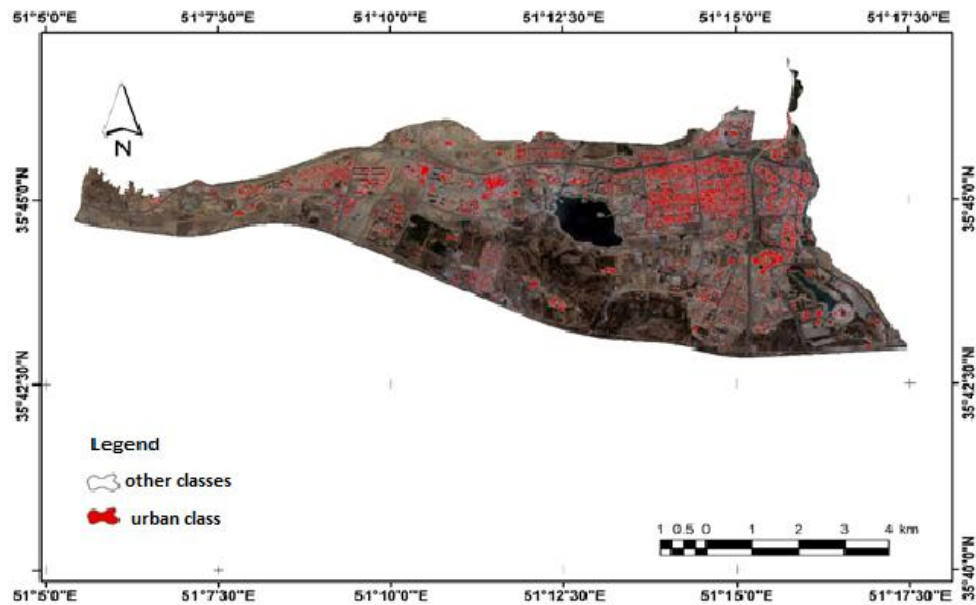

Fig. 2. Maximum likelihood classification [14]

Fig. 3. Construction area in 2018

Table 2. Sentinel 2 characteristics [17]

Spatial resolution (meters)	Average wavelength (µm)	Band name	Band number
60	0/43	Coastal aerosol	1
10	0.49	Blue	2
10	0/56	Green	3
10	0.65	Red	4
20	0/7	Vegetation Red Edge	5
20	0/74	Vegetation Red Edge	6
20	0/76	Vegetation Red Edge	7
10	0/84	NIR	8
20	0/86	Narrow NIR	8A
60	0.92	Water vapor	9
60	1/37	SWIR – Cirrus	10
20	1/61	Short-wave infrared	11
20	2/19	SWIR	12

Also, in Fig. 6, the trend of time changes of the AI index per time unit is displayed. Based on the obtained results, the amount of this pollutant has not grown much during this period of time, and it can be said that construction has not had a great impact on AI pollutant. Carbon monoxide as one of the most dangerous gases for human life demonstrated in Fig. 7 and 8 maps of pollutant changes.

As shown in Fig. 7, the amount of this pollutant in the eastern parts where there is more construction is higher than other areas . This increase in amount can be caused by more constructions in the eastern parts of the 22nd

district of Tehran. Fig. 8 demonstrated the changes in the carbon monoxide pollutant. Based on the results, it can be seen that since 2020, the intensity of this gas in the air has increased and it has experienced higher peak points. In Fig. 9, the trend of changes in nitrogen dioxide gas is shown spatially. According to the map, the concentration of these gases was very high in the eastern parts, especially the southeast. It can be normal due to the existence of more structures in these places. Also, in Fig. 10, the trend of time changes of this pollutant is shown. Based on the results, there is no specific trend between the changes of this pollutant with the increase in construction.
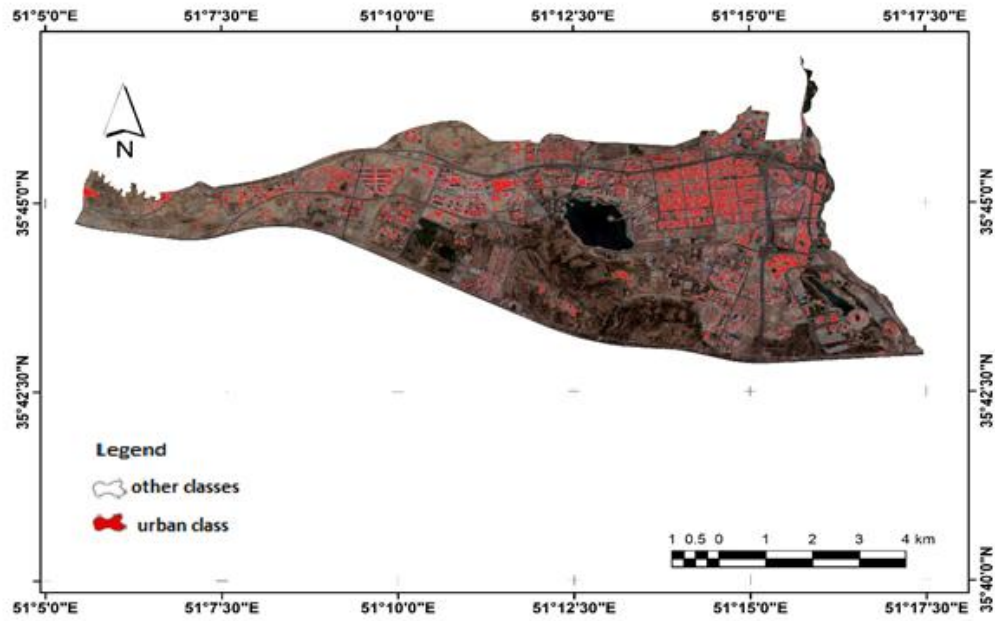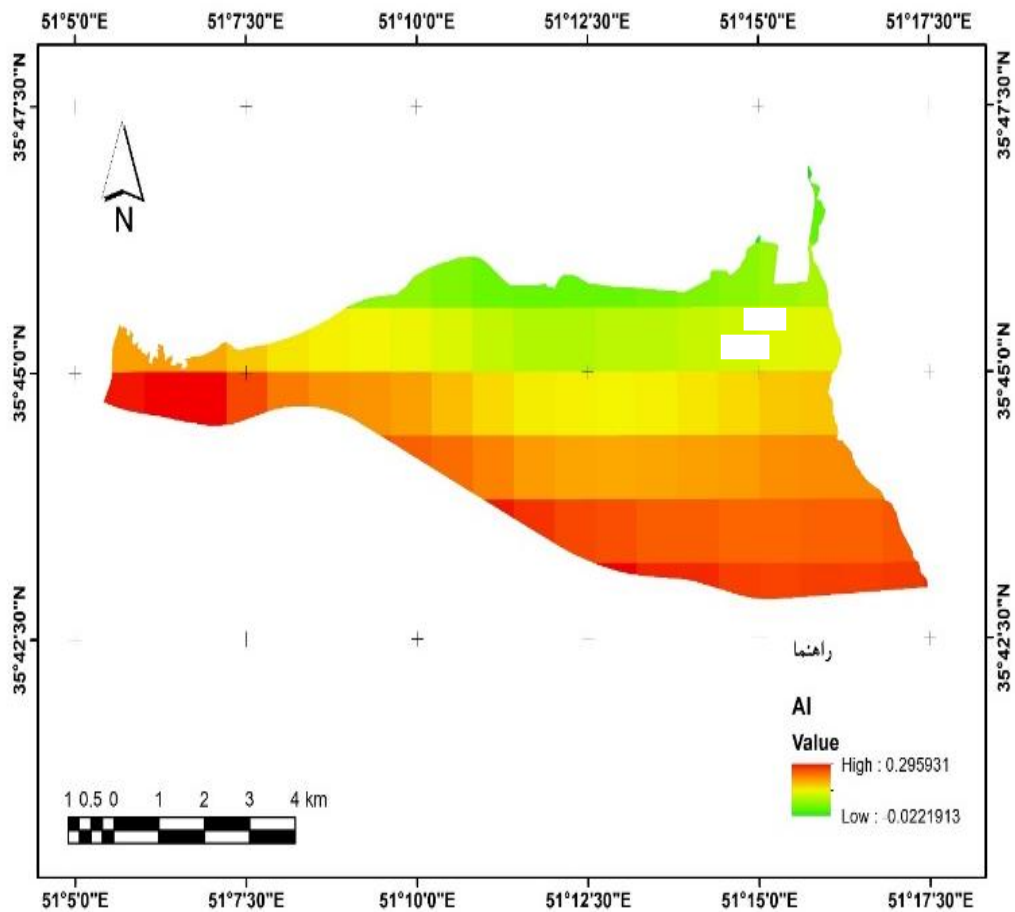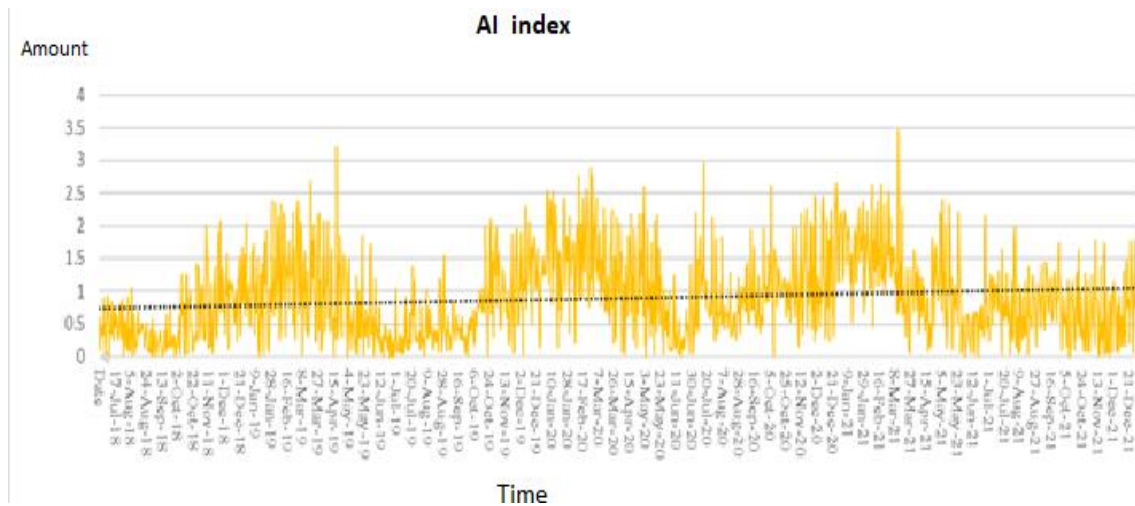
Fig. 4. Construction area in 2022

Fig. 5. AI index spatial changes

Table 5. Seasonal changes of air contaminators during study period

	2018	2019	2020	2021
CO				
Spring		0.033963	0.034625	0.0338
Summer	0.032966	0.034516	0.032941	0.034103
Autumn	0.031458	0.032406	0.033988	0.035472
Winter	0.03704	0.038291	0.042483	0.044744
So2				
Spring		0.000133	0.00012	0.000102
Summer		0.000113	9.91E-05	6.25E-05
Autumn		0.00031	0.000153	0.00033
Winter	0.001	0.00054	0.000804	0.000564
No2				
Spring		0.00035	0.000198	0.000188
Summer	1.25E-05	3.48E-05	8.93E-06	8.62E-06
Autumn	0.000391	0.000398	0.000549	0.000752
Winter	0.001263	0.000959	0.001079	0.001595
O3				
Spring		0.14783	0.142895	0.13893
Summer		0.126765	0.123158	0.127397
Autumn	0.124851	0.125737	0.121868	0.125667
Winter	0.129969	0.13641	0.142965	0.135324
AI				
Spring		0.88007	1.086904	1.063826
Summer	0.279925	0.324678	0.652886	0.167759
Autumn	0.454324	0.722061	1.062167	0.349596
Winter	0.905526	1.131429	1.494769	1.193955

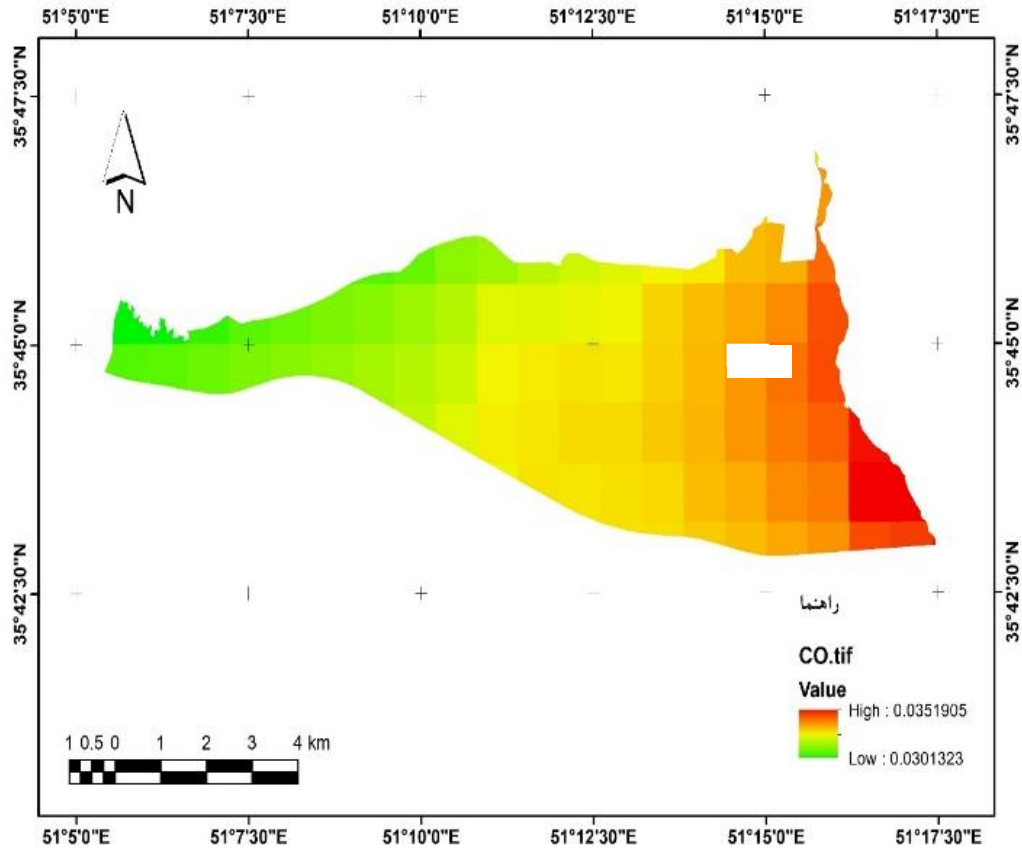**Fig. 6. The trend of changes in the AI index per unit of time**

Table 3. Accuracy coefficients

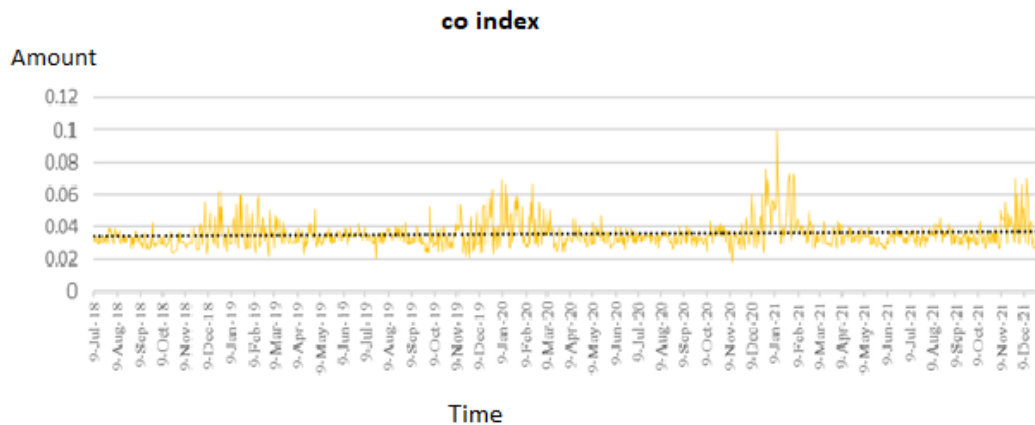| Year	Overall accuracy	Kappa coefficient
2018	0/91	0/84
2022	0/93	0/86

Table 4. Construction area changes

Year	Area (hectares)
2018	348/88
2022	382
The difference between two time periods	33/12

Fig. 7. CO index spatial changes map

Fig. 8. The trend of changes in the CO index per unit of time

Based on the results in Fig. 12, a significant increase of this pollutant in the eastern and western parts. Also, the change graph of this pollutant per time unit is displayed. In time changes, from 2021, a growing trend of this gas inside the region is obvious.
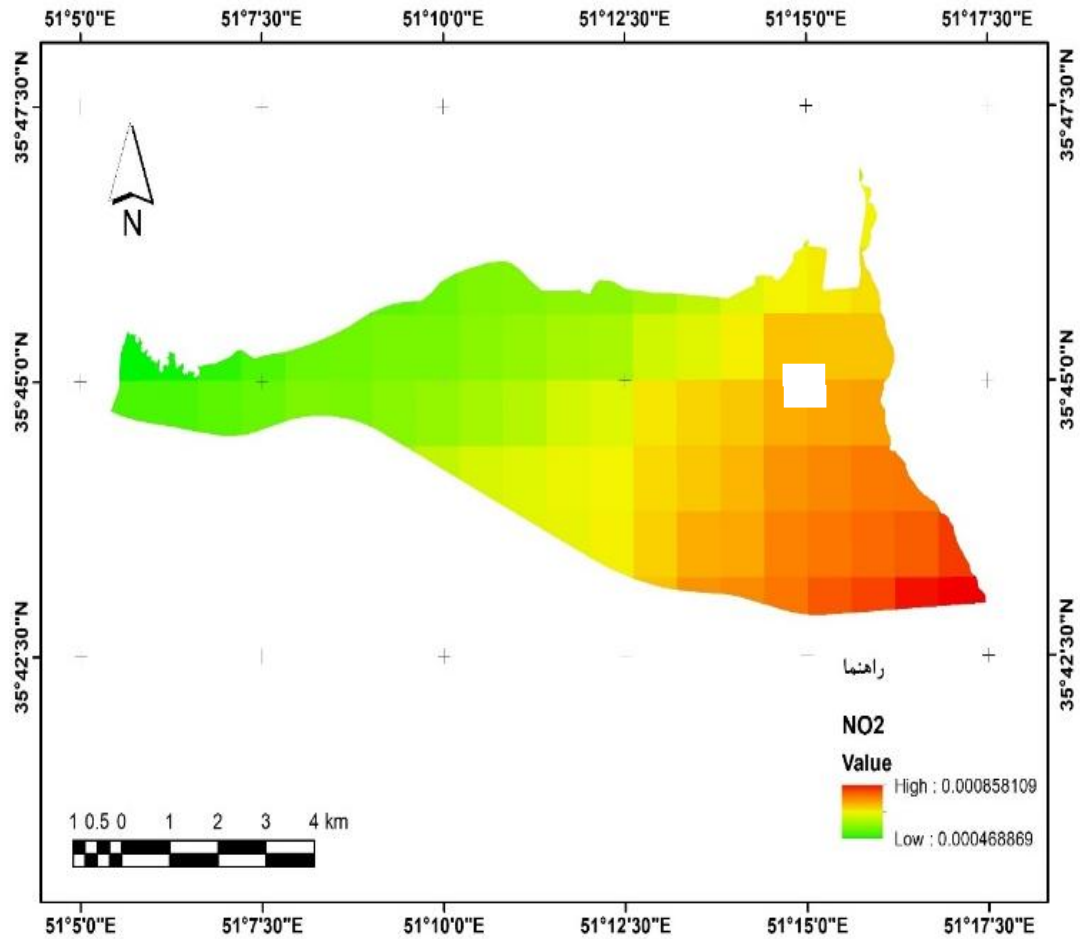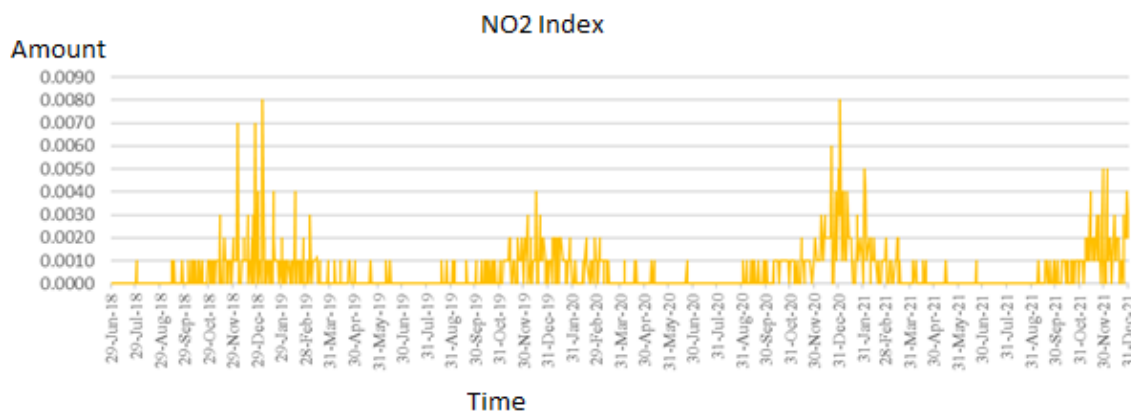
Fig. 9. NO2 index spatial changes map

Fig. 10. The trend of changes in the NO2 index per unit of time

Fig. 13 shows the spatial changes of O3 gas. According to the obtained results, the concentration of soot gas was more intense in the western and southwestern parts.

Fig. 14 demonstrated the trend of ozone pollutant changes over time. Based on this graph, no significant trend has been observed between the increase in construction and the ozone layer. The trend of seasonal changes for the mentioned 4 years exhibited in Table 5. For carbon monoxide gas, a growing trend of this pollutant is observed throughout the season. For sulfur dioxide gas, no logical and noticeable trend is observed. For the

nitrate dioxide pollutant, a growing trend in the concentration of this gas is observed in all seasons with the increase in construction. No logical trend has been observed for ozone gas either. In terms of the amount of aerosol, a growing trend is observed in different seasons during different years. Analysis of air pollution data has been done, which was obtained from the country's air quality monitoring system, which is a document for comparison and validation.
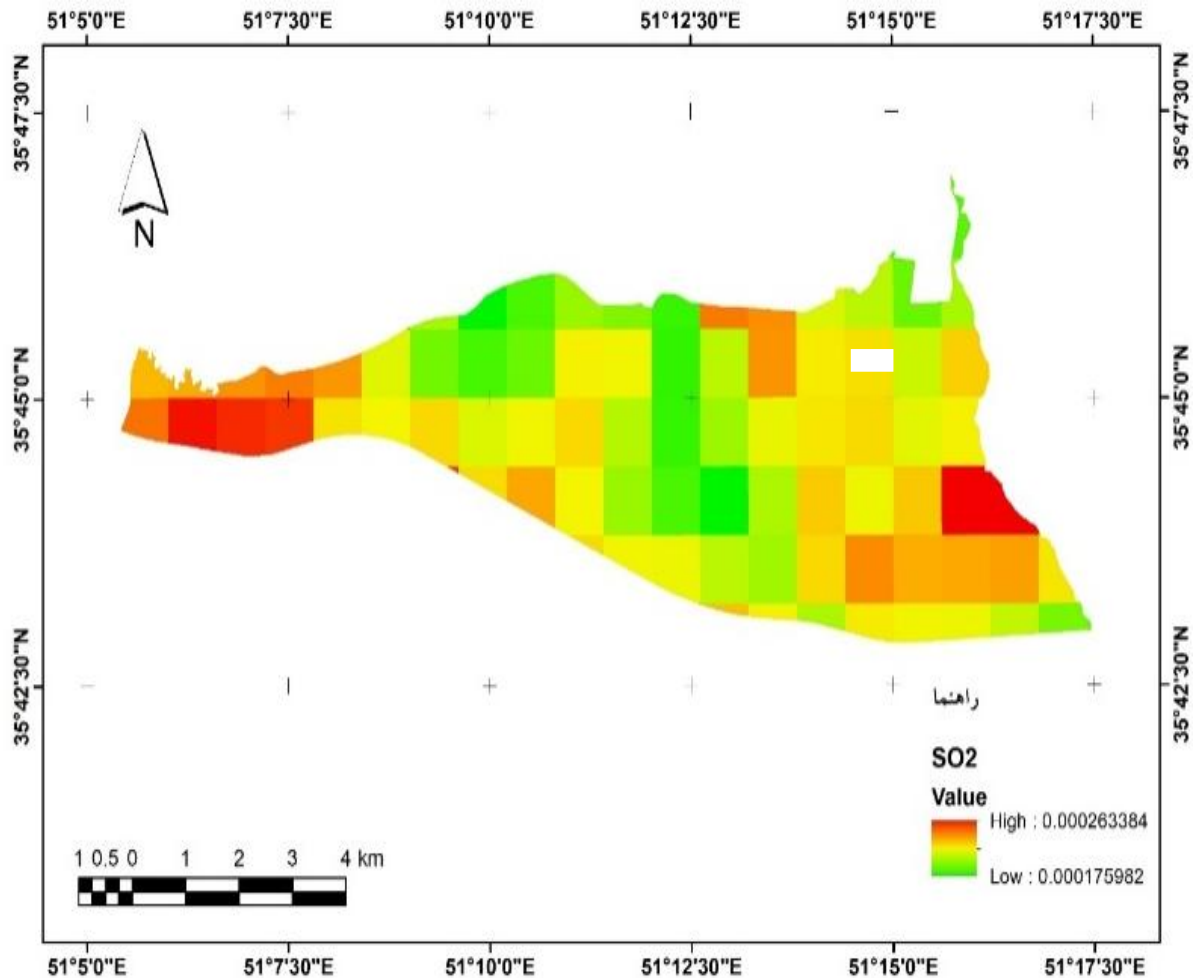

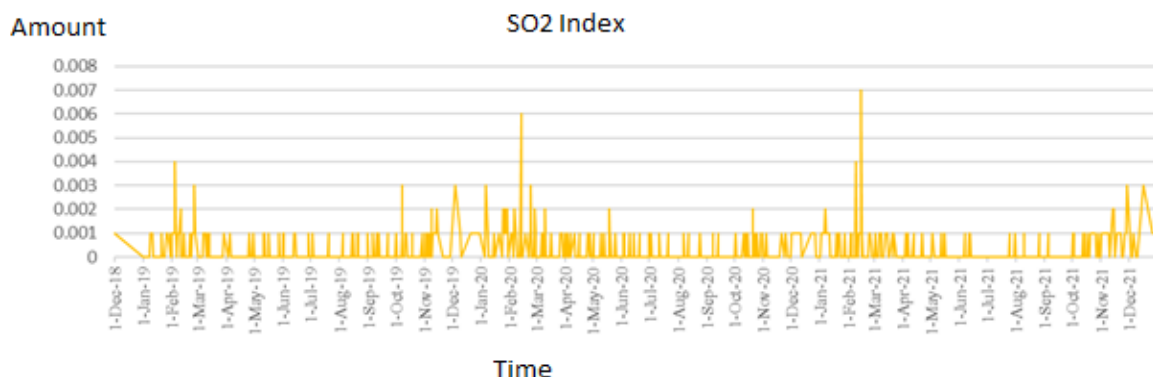
Fig. 11. SO2 index spatial changes map

Fig. 12. The trend of changes in the SO2 index per unit of time
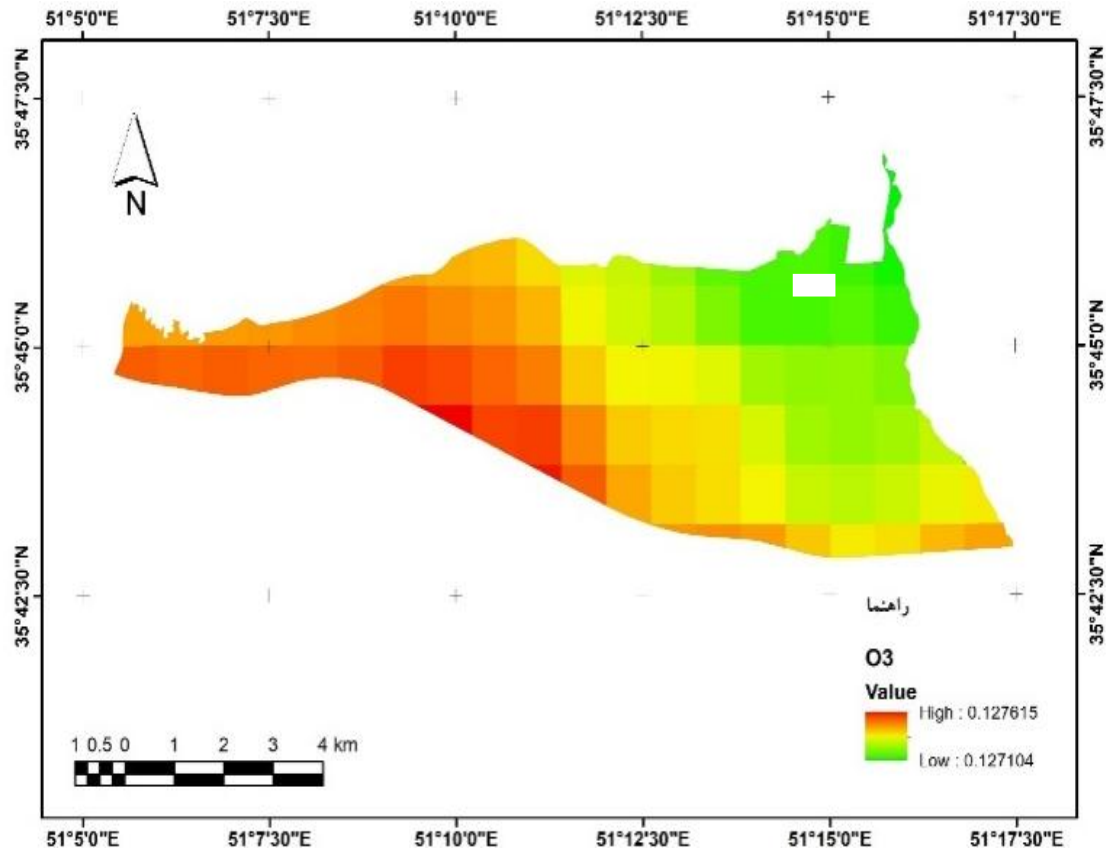
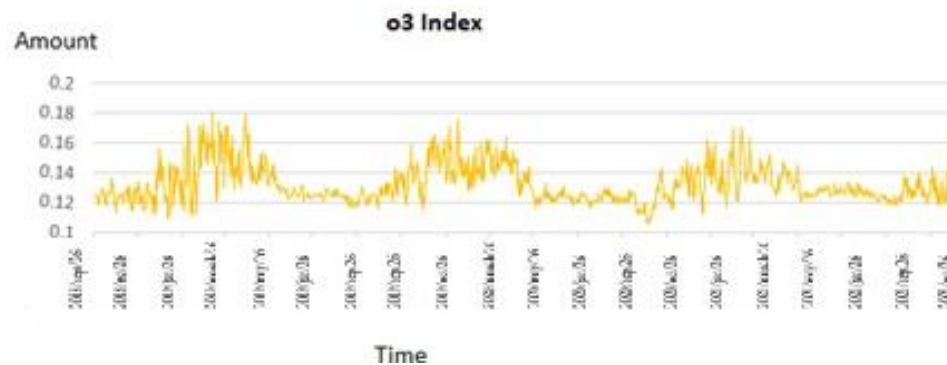**Fig. 13. O3 index spatial changes map**

Fig. 14. The trend of changes in the O3 index per unit of time

4. CONCLUSION

Air pollution is one of the parameters that has many spatial and temporal changes. These many changes of these parameters and its many disadvantages, the lack of ground stations with appropriate time and place distribution, have led us to other sciences. Perhaps the most important science that helps us in this field is remote sensing. Remote sensing is the science of obtaining information about objects and phenomena on the surface of the earth without

direct contact with them. Considering the unique features of remote sensing, i.e. reproducibility, comprehensiveness, access to past data, not being dependent on geographical boundaries can be very helpful in the discussion of air pollution. Based on the review of the changes obtained for construction in 2018, it was equal to 348.88 hectares, and in 2022, area was equal to 382 hectares. During these 4 years, 33 hectares have been added to the construction of the area. Examining the spatial changes of pollutants in the areas where there was more construction,

69

the amount of pollutants was also higher. In terms of time, however, no special changes have been observed for all gases. For AI pollutant, no very specific changes were observed within the region. We have seen a growing trend for carbon monoxide pollutant. For the nitrogen oxide pollutant, we have not seen any growth during this period of time. For sulfur dioxide, we have seen a growing trend. We have not seen a growing trend for the pollutant. Also, in terms of seasonal changes, air pollutants are more concentrated in winter.

COMPETING INTERESTS

Authors have declared that no competing interests exist.

REFERENCES

1. Available: https://earthengine.google.com/
2. Amani A. Et al. Google earth engine cloud computing platform for remote sensing big data appli, ieee. 2020;
3. Butt MJ, Assiri ME, Ali MA. "Assessment of AOD variability over Saudi Arabia MODIS deep blue products. In, environmental pollution. 2020;
4. Tan R, Liu Y, Liu Y, He Q, Ming L, Tang S. "Urban growth and its determinants across the Wuhan urban agglomeration, central China. Habitant Int. 2014;44:268-281.
5. Rangzen K. M. Temporal-spatial survey of nitrogen dioxide pollution in Khuzestan province using TROPOMI sensor, department of remote sensing and GIS, faculty of earth sciences, Shahid Chamran Univerity, Ahvaz ,Iran. 2019;
6. Shami Siavash et al. "Investigating the amount of changes in air pollutants during the spread of the Covid-19 virus in Iran using Sentinel 5 satellite data. Scientific Research Journal of Mapping Sciences and techniques. 2019;146-135.
7. Beniot Parmentier et al. Spatiotemporal data on the air pollutant nitrogen dioxide derived from sentinel satellite for France. 2020;
8. A. Z, Kaplan G. Relationship between pollutants, geographical and demographic data. International Journal of Engineering and Geosciences. 2020;
9. Antoine Lefebvre et al. Monitoring urban areas with sentinel-2a data: Application to the update of the copernicus high resolution layer imperviousness degree, CNES, UMR 6074 IRISA, OBELIX Team, Vannes 56000, France. 2016;
10. G. K, J. Chormański. Sentinel-2 imagery for mapping and monitoring imperviousness in urban areas, Warsaw university of life sciences, Faculty of civil and environmental engineering. 2019;
11. M. Krupiński et al. One class SVM for building detection on Sentinel-2 images. 2019;
12. Behrouz, Vahid S, Mohammad H. Y, Mohammadkia K. Monitoring, analysis and spatial and temporal zoning of air pollution (Carbon monoxide) using Sentinel-5 satellite data for health management in Iran, located in the Middle East, air quality, atmosphere & health. 2020;
13. Shami Siavash, Khoshlohjeh Azar Mehdi, Ghorbani Zahra, Moghimi Armin, Mohammadzadeh Ali, Sabetghadam Sayedah Samaneh. Investigating the amount of changes in air pollutants during the spread of the Covid-19 virus in Iran using Sentinel 5 satellite data. Scientific Research Journal of Mapping Sciences and Techniques. 2019;10(3):146-135.
14. Available: www.wikipedi.org
15. S. J, "Thematic validation of high-resolution global land-cover data sets. 1999;1051-1060.
16. Jensen, "Introductory digital image processing: A remote sensing perspective, 1996;
17. Alavi Panah A et al. "Application of remote sensing in earth sciences soil sciences. 2013;
18. Available:https://sentinels.copernicus.eu/web/sentinel/missions/sentinel-5/instrument-payload
19. Available:https://sentinels.copernicus.eu/web/sentinel/missions/sentinel-5/instrument-payload
20. Available:https://gisgeography.com/sentinel-2-bands-combinations/